Наносистеми, наноматеріали, нанотехнології
Nanosistemi, Nanomateriali, Nanotehnologii
2022, т. 20, № 1, сс. 145–158

PACS numbers: 75.50.Tt, 81.05.Zx, 81.07.-b, 81.16.-c, 81.20.Fw, 81.20.Ka

An Overview of Iron Oxide Nanoparticles: Characterisation, Synthesis, and Potential Applications

Ayad Mohammed Nattah[1] and Ahmed Hashim[2]

[1]*College of Materials Engineering,*
Department of Physics,
University of Babylon,
Hillah, Iraq
[2]*College of Education for Pure Sciences,*
Department of Physics,
University of Babylon,
Hillah, Iraq

Iron oxide nanoparticles have gained recently much attention due to their outstanding applications including gas sensors, catalysis, optical magnetic recording, electronic devices, and biomedical applications. Different methods have been employed in order to generate iron oxide nanoparticles of required size and morphology to use potentially in many field sectors. In this review, summaries of importance, structure and properties of Fe_2O_3 nanoparticles are demonstrated. Recently, a number of researchers have been developed synthesis methods for obtaining iron oxide nanoparticles, which are classified into basic methods: physical, chemical and biological syntheses. A detailed overview of different applications for iron oxide nanoparticles is presented.

Наночастинки оксиду Феруму останнім часом привернули велику увагу завдяки своїм видатним застосуванням, що включають газові датчики, каталізу, оптичний магнетний запис, електронні пристрої, а також біомедичні застосування. Різні методи були використані для того, щоб ґенерувати наночастинки оксиду Феруму необхідного розміру та морфології для потенційного використання в багатьох секторах поля діяльности. У цьому огляді продемонстровано резюме важливості, структури та властивостей наночастинок Fe_2O_3. Останнім часом ряд дослідників розробили методи синтези одержання наночастинок оксиду Феруму, які класифікуються на основні методи: фізична, хемічна та біологічна синтези. Представлено детальний огляд різних застосувань для наночастинок оксиду Феруму.

Key words: iron oxide, nanoparticles, nanofabrication, characterisation.

Ключові слова: оксид заліза, наночастинки, вироблення, характеризація.

(Received 21 April, 2021; in revised form, 26 April, 2021)

1. INTRODUCTION

Nanotechnology has greatly contributed in several fields of research and considered as a gate of the revolutionary technology in the 21st century. This technology has seen recently an emerging area of science and become a powerful tool for new nanosize particles and their applications [1]. The science of nanotechnology includes the controlling of atoms and molecules for creating new materials with different useful applications in various fields [2]. Nanomaterials have gained a great deal of attention due to their excellent optical, electrical, magnetic, and catalytic properties. As well known, the nanomaterials' properties and their potential applications have significant influence by means of phases, sizes, and morphologies. Thus, much attention has been paid for synthesis of nanostructured materials with controlled and novel morphologies [3].

Iron oxide nanoparticles at a size range 1–100 nm have gain a great deal of interest due to its unique magnetic properties, which have a great impact in electronics, medicine, and modern science. Iron oxide is defined as mineral compound and shows different polymorphic forms including maghemite (γ-Fe_2O_3), hematite (α-Fe_2O_3) and magnetite (Fe_3O_4) [4]. The iron oxide at nanoscale have been widely applied in different potential applications such as solar cells [5, 6], pigments and paints [7], gas sensors [8], photocatalyst [9–11], fuel cell [12, 13], optical fibres and telecommunication [14, 15], future lithium batteries [16], biosensors [17], photo-detectors [18], sequestration of pollutants [19], drug delivery [20, 21].

Iron oxide nanoparticles are commonly produced by using two main methods: top-down and bottom-up method. Top-down route involves mainly physical methods, whereas bottom-up routes mainly include chemical and biological methods for fabrication of the nanoparticles [22]. Chemical methods are the most decisive methods in widely applied production of iron oxide nanoparticles. The most common chemical methods are such as hydrothermal, sol–gel, microwave, co-precipitation, *etc*. However, the preparation procedures are too complex and generally required high temperatures [23, 24]. To overcome these limitations, it has been recently flame synthesis, which has a great benefit comparing with wet chemical methods [25]. This method has shown to be an economic, easy, simplest, scalable process suitable for achieving high production rates [26].

There are two basic routes employed to produce the nanoparticles, which are classified into bottom-up and top-down ones. The bottom-up route involves gas-phase and liquid-phase methods. In the literature, the bottom-up approach includes a variety of synthesis methods to pro-

duce the nanoparticles such as hydrothermal, co-precipitation, sol–gel, microwave, *etc*. However, the limitations and drawbacks of these methods in term of cost, efficiency and complexity are great challenge [23, 24]. As proven in recent year, gas-phase processes can be considered as one of the most effective ways to generate nanoparticles. This approach possesses advantages including large scale-production, single-step and continuous process, high purity of products. Moreover, it does not involve all the extensive steps related to wet-chemistry methods [25, 26]. Flame synthesis has enormous valuable comparing the wet chemical processes [25]. Combustion synthesis is the cost effective method and has become simplest route for fabrication of the nanoparticles. Generally, flame synthesis occurs as a single-step process, while wet chemical methods take multiple steps. Most importantly, combustion synthesis has proven to be an easily scalable process that can achieve high product yields and large continuous production quantity [26].

2. SYNTHESIS METHODS OF IRON OXIDE NANOPARTICLES

The most common approaches for producing iron oxide nanoparticles are including physical, chemical and biological ones. The selection of each method of synthesis has significant influence on producing iron oxide with a desired size, shape, structure and magnetic properties. The main approaches to synthetize iron oxide nanoparticles, highlighting advantages and limitations of each technique are as follow [4].

2.1 Chemical Methods

2.1.1. Sol–Gel

Sol–gel processing and a wet chemical-synthesis approach are widely used to synthesize magnetic nanoparticles. In this method, the process starts with a chemical solution as precursor undertake different forms of hydrolysis and polycondensation reactions. The solution is then stirring to make a sol. The sol is then dried to form a gel by using chemical reaction. The basic catalysis leads to producing a colloidal gel, while a polymeric form of the gel is produced by means of acid catalysis. The particles produced in this method are significantly influenced by the rate of condensation and hydrolysis. The set of solvent parameters, namely, concentration, pH, and temperature, have impact on the size of the particles too [27, 28].

2.1.2. Hydrothermal Synthesis

The hydrothermal synthesis methods can be described as any heteroge-

neous reactions for synthesizing inorganic materials. The process is carried out by using aqueous solution above ambient temperature above 200°C and higher pressure more than 2000 psi [29]. In this method, the experimental procedure involves dissolving the reactants in the water. Then, the solvent will be heated above the boiling point for the desired duration [30].

The nanoparticle size increases, when both the amount of water and the time of reaction increase.

2.1.3. Co-Precipitation

The co-precipitation method is the most commonly used as promising route for generating iron oxide nanoparticles. This method has many advantages such as simplicity, productivity, requires less procedures and hazardous materials, and, therefore, become widely employed for biomedical applications. The production of the iron oxide nanoparticles is undertaken by an ageing of stoichiometric mixture of ferric salts and ferrous in aqueous media [31]. Nanoparticle size, shape, and composition influence significantly on the used salts, the pH of the solution, the temperature, the ratio of Fe^{2+} and Fe^{3+}, and the media ionic strength. Generally, this method is low cost and becomes much convenient for a very high production rate. However, the great challenge is in the nanoparticles involving their aggregation and large size distribution [32].

2.1.4. Microwave Method

Microwave method has gain much interesting due to simpler, low cost, a shorter crystallization time, and more energy efficient technique to synthesize new improved nanostructural materials and short crystallization time comparing with the conventional heating methods [33]. Therefore, microwave method is a convenient technique for preparing nanocrystalline oxides with possible formation of new metastable phases and rapid heating to reach the required temperature. The microwave route has been developed by Mohammadi *et al.* [34] for preparing iron oxide nanoparticles. In this method, the experimental reaction happens by mixing a solution of starting materials $Fe(NO_3)\cdot 2.9H_2O$ and urea. Then, the irradiation process for the mixed solution takes place under 540 W microwaves for 6 min. Finally, the calcination process undertakes for the prepared sample at 800°C for 4 hours to obtain the Fe_2O_3 nanoparticles.

2.2. Physical Method

The nanoparticles can be generated by using a number of physical methods including laser ablation, chemical vapour decomposition,

plasma synthesis, and combustion synthesis. However, the most important challenge with this method is the inability for controlling the particle size in the nanometre range [35].

2.2.1. Gas-Phase Deposition

This route involves both chemical vapour deposition (CVD) and physical vapour deposition. In this method, iron is a raw material and is used as metal for production of different products and outcome. The physical vapour deposition method is unique to form the composite and thin film of nanoparticles. In this method, the particles' formation takes place because of the consolidation due to thermal treatment of composites onto a surface. In addition, the particles' formation takes place because of the supersaturation precursor molecules in the gaseous phase. The CVD method has many advantages in case of producing the large scale and quality thin films and nanotube of iron oxide. Besides, the produced particles by gas-phase deposition are commonly of high purity comparing with liquid-based synthesis. However, the most important challenge with gas-phase deposition technique is the risk of contamination [36].

2.2.2. Thermal Decomposition

Thermal decomposition is effective and easiest route for generating iron oxide nanoparticles. This method is based on the high-temperature thermal decomposition of organometallic or coordinated iron precursors in organic solvents to obtain the iron oxide nanoparticles. In this method, the organometallic compound is used as precursor molecules, and heating it leads to the production of iron oxide nanoparticles. Then, the heating process of the precursor causes decomposition of the iron oxide molecules. Iron oxide nanoparticles are produced at outstanding quality and size range about 15 nm. However, the method of thermal decomposition frequently involves complicated precursor synthesis, requires high temperatures and inert conditions [37].

2.2.3. Ball-Milling Method

The ball milling is a simplest and inexpensive mechanical technique for producing iron oxide nanoparticles from the bulk. In this method, reducing the size of the larger particles is undertaken by impact as the balls drop from near the top of the shell. The ball milling method is efficient to produce of different-type nanoparticles on an industrial scale. The nanoparticles produced are uniform and small sized and exhibit different properties [38].

2.2.4. Pyrolysis

The pyrolysis method is most commonly used for synthesis of nanoparticles. This method has many advantages and outstanding due to the cost-effective, efficient, simple, continuous process. The reaction takes place in this method, when the precursor (liquid or vapour) burn with the flame. Then, at high pressure, the precursor is transferred into furnace that leads to recover nanoparticles. It can be improved in the evaporation process by using plasma or laser instead of flame in order to reach high temperatures [38].

2.2.5. Laser Ablation

Advanced laser ablation is a promising approach for synthesizing different types of nanoparticles from various solvent. However, the agglomeration and controlled size distribution are the great challenges. This method is efficient to produce various types of the nanoparticles such as nanowires, carbon nanotubes, quantum dots, semiconductor and core–shell nanoparticles. The production of the nanoparticles is based on the growth and nucleation of laser-vaporized species. The nanoparticles produced by laser ablation have high purity due to the high purity of the target and ambient media in state of gas or liquid, which are not contaminated from the reactor [39]. The formation mechanism in laser ablation technique is based on the removal of surface atoms of the iron precursor. The process takes place by focusing the laser beam on the surface of a solid target material. The ambient media used is gas or liquid. Then, the vaporizing target material takes place due to rapidly increasing the irradiation temperature [36, 39].

2.2.6. Combustion

Combustion synthesis has become most important route for synthesis of inexpensive metal oxide nanoparticles. This method has advantages in terms of single-step process, high purity, simplest and continuous production. This method is more effective route and widely used over wet chemical approaches. Thus, flame synthesis has been successfully applied in the synthesis of iron oxide nanoparticles. In this method, the flames produce high temperatures that important to activate precursor pyrolysis.

The final product obtained has outstanding characteristics including controlled particle size distribution, phase and composition. The nanoparticles' properties are highly affected by the altering flame operating conditions: temperature, reactant concentration, stoichiometry, pressure, burner configuration, precursor injection location [40, 41].

2.3. Biological Methods

This method has been applied for large production of iron oxide nanoparticles that is based on biological sources such as bacteria, fungi, plant extracts and protein-mediated ones. This technique has many advantages in term of eco-friendly, simple, cost effective. However, the characteristics of the particles produced are less stable, non-uniform, and agglomerated. There are various part of plant can be used to generate the nanoparticles such as leaf, stem, root, and fruit. In addition, bacteria have excellent ability to reduce the metal ions and, therefore, are utilized for producing metallic and other novel nanoparticles. Furthermore, fungi are considered as very efficient method to produce metal oxide nanoparticles [36].

3. NANOPARTICLE TYPES, STRUCTURE AND APPLICATIONS

Iron oxide nanoparticles can be found in the three main form such as hematite (α-Fe_2O_3), maghemite (γ-Fe_2O_3), and magnetite (Fe_3O_4). Iron oxide has different crystal structures, which can be described in terms of iron cations and oxygen anions in tetrahedral or octahedral interstitial sites. For instance, the arrangement of the oxygen ions in hematite are found in a hexagonal close-packed lattice, whereas, Fe(III) ions occupy octahedral sites. The arrangement of oxygen ions in maghemite and magnetite is in a cubic close-packed structure. In magnetite, Fe(III) ions are distributed randomly between tetrahedral and octahedral sites and have inverse spinal structure [36].

Figure 1 shows the crystal structure of the three kinds of iron oxide.

Nanoparticles size, shape and synthesis method play a vital role in the nanoparticles properties. Therefore, the nanoparticles are exhibit outstanding optical, chemical, magnetic, and magnetic properties as results

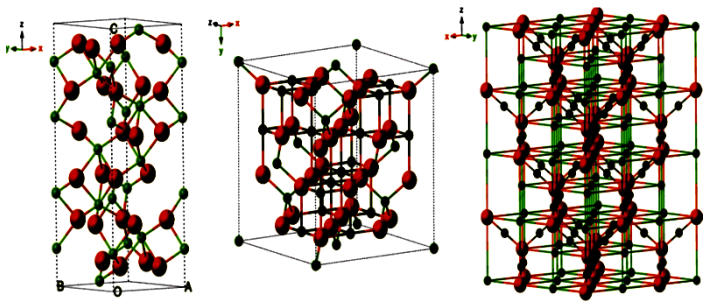

Fig. 1. The crystal structures of hematite, magnetite and maghemite [33].

Properties	Magnetite (Fe_3O_4)	Maghemite (γ-Fe_2O_3)
Density (g/cm^3)	5·18	4·87
Melting point (°C)	1583–1597	—
Hardness	5·5	5
Type of magnetism	Ferromagnetic	Ferromagnetic
Curie temperature (K)	850	820–986
M_s at 300K (A-m^2/kg)	92–100	60–80
Standard free energy of formation $\Delta G_f°$ (kJ/mol)	−1012·6	−711·1
Crystallographic system	Cubic	Cubic or tetrahedral
Structural type	Inverse spinel	Defect spinel
Space group	Fd3m	$P4_332$ (cubic); $P4_12_12$ (tetragonal)
Lattice parameter (nm)	a = 0·8396	a = 0·83474 (cubic); a = 0·8347, c = 2·501 (tetragonal)

Fig. 2. The main physical properties of iron oxides [43].

of the nanosize effects. The size diameter less than 20 nm exhibit superparamagnetic behaviour that is more suitable for biomedical applications [23]. The morphology and distribution of particle size are also having significant impact on the characterization of nanoparticles [42].

The main properties of nanoparticles including physical, optical and magnetic properties are demonstrated in Fig. 2.

4. POTENTIAL APPLICATION OF NANOPARTICLES

Nanomaterials at nanoscale size ranging from 1 to 100 nm are exhibit unique properties of materials. Iron oxide nanoparticles have received considerable attention due to its possessing unique advantages over other materials. Iron oxide nanoparticles have many attractive physical and chemical properties because of their nanoscale size. Thus, the nanoparticle has become most important in many technological fields and highly promising for a wide range of applications such as solar cell, catalysis, electronics, energy storage, gas sensor, and biomedical applications [44, 45]. The range of applications of nanoparticles in the different areas is shown in Table.

5. CONCLUSION

Iron oxide nanoparticles are potentially employed in many industrial sectors that enable technology for a variety of practical applications. The nanoparticles' properties and their diverse applications are significantly influenced by nanomaterials' sizes, shape and structure.

TABLE. Applications of iron oxide nanoparticles.

Type and Size of Iron Oxide	Application	Characterizations	Refs.
Fe_3O_4 (400 nm)	Wastewater treatment	Fe_3O_4 coating with silica employed as composite microspheres potentially exhibit recyclable tool for heavy metal ion removal from industrial wastewater	[46] Hu *et al.*, 2010
Maghemite Fe_2O_3 (15 nm)	Wastewater	γ-Fe_2O_3 coating with an inorganic feroxyhyte layer to improve surface properties of Fe_2O_3; as a result, enhance removing of Cr(VI) from synthetic wastewater	[47] Hu *et al.*, 2007
γ-Fe_2O_3, Fe_3O_4 hollow microspheres at 5 nm	Wastewater	γ-Fe_2O_3 and Fe_3O_4 are good adsorbents for different types of organic pollutants such as salicylic acid, methylene blue, and basic fuchsine in water; thus, its potentially applied in the waste water treatment	[48] San Xu *et al.*, 2012
Superparamagnetic iron oxide nanoparticles (SPIONs) (20 nm or less)	Biomedical	SPIONs is successfully used for diagnosing the liver and spleen cancers in MRI diagnostics by active targeting methods by allowing longer effective imaging times	[49] Rosen *et al.*, 2012
Monodisperse hollow Fe_2O_3 nanoovals (40–80 nm)	Photocatalysis and gas sensors	Monodisperse hollow magnetic Fe_2O_3 exhibit excellent properties on photocatalytic decomposition of salicylic acid; also, shows a good response for detecting trace level of ethanol	[50] Zhong *et al.*, 2010
Powder of maghemite Fe_2O_3 at average size range (35, 100, 150 nm)	Photocatalytic	The crystallite size of iron oxides at 35 and 150 nm causing complete decomposition of Congo red dye, whereas iron oxide particles at 100 nm have not ability for decomposition the dye	[51] Khedr *et al.*, 2009

Continuation **TABLE.**

Type and Size of Iron Oxide	Application	Characterizations	Refs.
α-Fe_2O_3 hollow microspheres (6–8 nm)	Photocatalysts	The designed hollow microsphere showed potential applications in photocatalysis; thus, it perfectly used due to their high conductivity, high photocurrent, and high photocatalytic activity	[52] Xu *et al.*, 2013
Nanosize alpha- and gamma-Fe_2O_3 (20–40 nm)	Environmental health	For algal species, α-Fe_2O_3 showed less toxicity than γ-Fe_2O_3 NPs undertaken a comparative analysis for two algal species, and the results shows more sensitive than nanochloropsis; the toxicity is confirm for food chain and environmental health	[53] Demir *et al.*, 2015
USPIO nanoparticles (NPs) at size diameter $\leq$ 50 nm	Clinical applications	USPIO nanoparticles are effective tool to detect brain tumours, monitoring treatment, and imaging treatment effects; also, can be used efficiently for evaluating tumour vascularity without requiring repeat injections due to its long circulation time	[54] Iv *et al.*, 2015
γ-Fe_2O_3 NPs (20 nm)	Solar cell	Magnetic γ-Fe_2O_3 NPs dispersed in titanium film for improving the performance of dye sensitized solar cells (DSSCs); the results showed that an optimal amount of 1.5 wt.% γ-Fe_2O_3 NPs, the DSSCs power conversion efficiency increased about 18% due to effecting of the magnetic field from γ-Fe_2O_3 NPs; this will lead to improve the ability of photogenerated electron transfer and also improve photovoltaic performances	[55] Cai *et al.*, 2016

Continuation **TABLE.**

Type and Size of Iron Oxide	Application	Characterizations	Refs.
Spherical iron oxide nanoparticles are around 20 nm in diameter	Cancer therapy	The horseradish peroxidase (HRP) in the nanoparticles has highly influence on the particle collected; the iron oxide entrapped with enzyme shows higher stability towards temperature change compared with free enzyme	[56] Gupta *et al.*, 2016
N-type semiconductor of α-Fe_2O_3 NPs 35–39 nm	Gas sensor	Outstanding employed for detection of explosive, toxic and harmful gases in industrial applications	[57] Naval, 2016
α-Fe_2O_3 with hollow spindles and solid spindles at size range 2–3 μm	Gas sensor	Hematite iron oxide with hollow spindle-like exhibits excellent response for organic gas such as acetone and 2-propanol; the porous hollow hematite spindles have large surface area and porous hollow structure and, therefore, shows excellent response for gas sensering	[58] Huang *et al.*, 2011
Uniform porous α-Fe_2O_3 nanostructures at 10.2 nm	Gas sensors and lithium storage in lithium ion batteries	Hematite iron oxide posses outstanding sensing responses against acetone, ethanol, methanol, butanol and isopropanol; therefore, its potentially used in flammable gases; the porous α-Fe_2O_3 exhibits excellent lithium storage capacity and considerably improved the capacityof retention; thus, can be widely used in the lithium ion batteries as anode materials	[59] Su *et al.*, 2012
Iron oxide nanoparticles of ultrafine size range 3–8 nm	Health effects and the environmental problems	Highly significant impact on both environmental problems and health effects due to higher removal capacity of methyl orange (MO) from waste water	[60] Lian *et al.*, 2009

This review provides an updated and critical focusing on nanoparticles, their classification, synthesis, providing examples of different practical applications. The nanoparticles have different applications in science such as electronics, solar cell, and biomedical field. A summary review of nanoparticles' synthesis including chemical and physical route is presented.

REFERENCES

1. A. Petri-Fink and H. Hofmann, *IEEE Trans Nanobioscience*, **6**, No. 4: 289 (2007); doi:10.1109/TNB.2007.908987
2. M. C. Roco, B. Harthom, D. Guston, and P. Shapira, *J Nanopart. Res.*, **13**, No. 7: 3557 (2011); https://doi.org/10.1007/s11051-011-0454-4
3. C. N. R. Rao, S. R. C. Vivekchand, K. Biswas, and A. Govindaraj, *Dalton Transactions*, **34**: 3728 (2007); https://doi.org/10.1039/B708342D
4. Z. Cheng, A. L. K. Tan, Y. Tao, D. Shan, K. E. Ting, and X. J. Yin, *International Journal of Photoenergy*, **2012**: Article ID 608298 (2012); https://doi.org/10.1155/2012/608298
5. X. P. Gao, J. L. Bao, G. L. Pan, H. Y. Zhu, P. X. Huang, F. Wu, and D. Y. Song, *J. Phys. Chem. B*, **108**, Iss. 18: 5547 (2004); https://doi.org/10.1021/jp037075k
6. A. Chowdhuri, V. Gupta, and K. Sreenivas, *Appl. Phys. Lett.*, **84**: 1180 (2004); https://doi.org/10.1063/1.1646760
7. P. Roth, *Proceedings of the Combustion Institute*, **31**, No. 2: 1773 (2007); https://doi.org/10.1016/j.proci.2006.08.118
8. K. J. Choi and H.W. Jang, *Sensors*, **10**, Iss. 4: 4083 (2010); https://doi.org/10.3390/s100404083
9. A. Santos, P. Yustos, A. Quintanilla, G. Ruiz, and F. Garcia-Ochoa, *Applied Catalysis B: Environmental*, **61**, Iss. 3–4: 323 (2005); https://doi.org/10.1016/j.apcatb.2005.06.006
10. A. Shah, N. Mittal, I. Bhati, V. K. Sharma, and P. B. Punjabi, *Polish Journal of Chemistry*, **83**, No. 11: 1959 (2009).
11. *Catalysis by Ceria and Related Materials*, *Catalytic Science Series* (Eds. A. Trovarelli and P. Fornasiero) (Imperial College Press: 2013), vol. **2**.
12. Z. Liu, L. M. Gan, L. Hong, W. Chen, and J. Y. Lee, *Journal of Power Sources*, **139**, Nos. 1–2 :73 (2005); https://doi.org/10.1016/j.jpowsour.2004.07.012
13. H. Zhu, X. Li, and F. Wang, *International Journal of Hydrogen Energy*, **36**, No. 15: 9151 (2011); https://doi.org/10.1016/j.ijhydene.2011.04.224
14. M. Tu, T. Sun. and K. Grattan, *Sensors and Actuators B*, **164**, No. 1: 1 (2012); https://doi.org/10.1016/j.snb.2012.01.060
15. A. Aubry, D. Y. Lei, S. A. Maier, and J. B. Pendry, *Phys. Rev. Letters*, **105**, No. 23: Article number 233901 (2010); https://doi.org/10.1103/PhysRevLett.105.233901
16. X. P. Gao. J. L. Bao, L. Pan, H. Y. Zhu, P. X. Huang, F. Wu, and D. Y. Song, *J. Phys. Chem. B*, **108**, No. 18: 5547 (2004); https://doi.org/10.1021/jp037075k
17. Md. M. Rahman, A. J. S. Ahammad, J. Jin, S. J. Ahn, and J. Lee, *Sensors*, **10**, No. 5: 4855 (2010); https://doi.org/10.3390/s100504855
18. S. B. Wang, C. H. Hsiao, S. J. Chang, K. T. Lam, K. H. Wen, S. Hung, S. J. Young, and B. R. Huang, *Sensors and Actuators A: Physical*, **171**, No. 2: 207

(2011); https://doi.org/10.1016/j.sna.2011.09.011
19. I. Ali, *Chem. Review*, **112**, No. 10: 5073 (2012); https://doi.org/10.1021/cr300133d
20. A. A. Manzoor, L. H. Linder, C. D. Landon, P. Ji-Young, A. J. Simnick, M. R. Dreher, S. Das, W. Park, A. Chilkoti, G. A. Koning, T. L. M. ten Hagen, D. Nadeen, and M. W. Dewhirst, *Cancer Res*, **72**, No. 21: 5566 (2012); doi:10.1158/0008-5472.CAN-12-1683
21. D. Sun, X. Zhuang, X. Xiang, Y. Liu, S. Zhang, C.Liu, S. Barnes, W. Grizzle, D. Miller, and Z. Huang-Ge, *Molecular Therapy*, **18**, Iss. 9: 1606 (2010); https://doi.org/10.1038/mt.2010.105
22. D. L. Huber, *Synthesis, Small Nano. Micro*, **1**, No. 5: 482 (2005); https://doi.org/10.1002/smll.200500006
23. Ibrahim Khan, Khalid Saeed, and Idrees Khan, *Arabian Journal of Chemistry*, **12**, Iss. 7: 908 (2019); https://doi.org/10.1016/j.arabjc.2017.05.011
24. W Zhi-Gang and G. Jian-Feng, *Micro & Nano Letters*, **7**, No. 6: 533 (2012); doi:10.1049/mnl.2012.0310
25. C. Li, Y. Hu, and W. Yuan, *Particuology*, **8**, No. 6: 556 (2010); https://doi.org/10.1016/j.partic.2010.08.009
26. K. Buyukhatipoglu and A. Clyne, *Journal of Nanoparticle Research*, **12**: 1495 (2010); https://doi.org/10.1007/s11051-009-9724-9
27. A. Tavakoli, M. Sohrabi, and A. Kargari, *Chemical papers*, **61**, No. 3: 151 (2007); doi:10.2478/s11696-007-0014-7
28. M. Tadic, D. Markovic, V. Spasojevic, V. Kusigerski, M. Remskar, J. Pirnat, and Z. Jaglicic, *Journal of Alloys and Componds*, **441**: 291 (2007); doi:10.1016/j.jallcom.2006.09.099
29. B. Mao, Z. Kang, E. Wang, S. Lian, L. Gao, C. Tian, and C. Wang, *Materials Research Bulletin*, **41**, No. 12: 2226 (2006); https://doi.org/10.1016/j.materresbull.2006.04.037
30. W. Wu, S. Yang, J. Pan, L. Sun, J. Zhou, Z. Dai, X. Xiao, H. Zhang, and C. Jiang, *Royal Society of Chemistry*, **16**, No. 25: 5566 (2014); https://doi.org/10.1039/C4CE00048J
31. W. M. Daoush, *Journal of Nanomedicine Research*, **5**, No. 3: 001118 (2017); doi:10.15406/jnmr.2017.05.00118
32. S. Riaz, M. Bashir, and S. Naseem, *IEEE Transactions on Magnetics*, **50**, No. 1: 4003304 (2014); doi:10.1109/TMAG.2013.2277614
33. W. Wu, Z. Wu, T. Yu, C. Jiang, and K. Woo-Sik, *Sci. Technol. Adv. Materials*, **16**, No. 2: 023501 (2015); https://doi.org/10.1088/1468-6996/16/2/023501
34. S. Z. Mohammadi, M. Khorasani-Motlagh, and S. Yousefi, *Int. J. Nanosci. Nanotechnology*, **8**, No. 2: 87 (2012); https://iranjournals.nlai.ir/handle/123456789/80012
35. J. Xu, J. Sun, Y. Wang, J. Sheng, F. Wang, and M. Sun, *Molecules*, **19**, Iss. 8: 11465 (2014); doi:10.3390/molecules190811465
36. A. V. Samrot, C. S. Sahithya, J. Selvarani, S. K. Purayil, and P. Ponnaiah, *Current Research in Green and Sustainable Chemistry*, **4**: 100042 (2021); https://doi.org/10.1016/j.crgsc.2020.100042
37. L. S. Arias, J. P. Pessan, A. P. M. Vieira, T. M. T. de Lima, A. Delbem, A. C. B. Delbem, and D. R. Monteiro, *Antibiotics*, **7**, Iss. 2: 46 (2018); doi:10.3390/antibiotics7020046
38. I. Ijaz, E. Gilani, A. Nazir, and A. Bukhari, *Green Chmistry Letters and Reviews*,

13, No. 3: 223 (2020); https://doi.org/10.1080/17518253.2020.1802517
39. M. Kim, S. Osone, T. Kim, H. Higashi, and T. Seto, *KONA Powder and Particle Journal*, **34**: 80 (2017); https://doi.org/10.14356/kona.2017009
40. S. E. Pratsinis, *Progress in Energy and Combustion Science*, **24**, Iss. 3: 197 (1998); https://doi.org/10.1016/S0360-1285(97)00028-2
41. M. S. Wooldridge, *Progress in Energy and Combustion Science*, **24**, Iss. 1: 63 (1998); https://doi.org/10.1016/S0360-1285(97)00024-5
42. S. L. Pal, U. Jana, P. K. Manna, G. P. Mohanta, and R. Manavalan, *Journal of Applied Pharmaceutical Science*, **1**, No. 6: 228 (2011).
43. C. Fu and N. M. Ravindra, *Bioinspired, Biomimetic and Nanobiomaterials*, **1**, No. 4: 229 (2012); https://doi.org/10.1680/bbn.12.00014
44. O. Kayser, A. Lemke, and N. Hernández-Trejo, *Current Pharmaceutical Biotechnology*, **6**, No. 1: 3 (2005); doi:10.2174/1389201053167158
45. C. N. R. Rao, G. U. Kulkarni, P. J. Thomas, and P. P. Edwards, *Chem. Soc. Reviews*, **29**, No. 1: 27 (2000); https://doi.org/10.1039/A904518J
46. H. Hu, Z. Wang, and L. Pan, *Journal of Alloys and Compounds*, **492**, Nos. 1–2: 656 (2010); https://doi.org/10.1016/j.jallcom.2009.11.204
47. J. Hu, I. M. C. Lo, and G. Chen, *Separation and Purification Technology*, **58**, No. 1: 76 (2007); https://doi.org/10.1016/j.seppur.2007.07.023
48. X. Jing-San and Z. Ying-Jie, *J. Colloid Interface Science*, **385**, No. 1: 58 (2012); doi:10.1016/j.jcis.2012.06.082
49. Joshua E. Rosen, Lorena Chan, Dar-Bin Shieh, and Frank X. Gu, *Nanomedicine: Nanotechnology, Biology and Medicine*, **8**, Iss. 3: 275 (2012); doi:10.1016/j.nano.2011.08.017
50. J. Zhong and C. Cao, *Sensors and Actuators B: Chemical*, **145**, No. 2: 651 (2010); https://doi.org/10.1016/j.snb.2010.01.016
51. M. H. Khedr, K. S. Abdel Halim, and N. K. Solima, *Materials Letters*, **63**, Nos. 6–7: 598 (2009); https://doi.org/10.1016/j.matlet.2008.11.050
52. L. Xu, J. Xia, K. Wang, L. Wang, H. Li, H. Xu, L. Huang, and M. He, *Dalton Trans*action, **42**, No. 18: 6468 (2013); https://doi.org/10.1039/C3DT50137J
53. V. Demir, M. Ates, Z. Arslan, M. Camas, F. Celik, C. Bogatu, and S. S. Can, *Bulletin of Environmental Contamination and Toxicology*, **95**, No. 6: 752 (2015); doi:10.1007/s00128-015-1633-2
54. M. Iv, N. Telischak, D. Feng, S. J. Holdsworth, K. W. Yeom, and H. E. Daldrup-Link, *Nanomedicine*, **10**, No. 6: 993 (2015); doi:10.2217/nnm.14.203
55. F. Cai, S. Zhang, and Z. Yuan, *RSC Advances*, **5**, No. 53: 42869 (2015); https://doi.org/10.1039/C5RA05936D
56. N. Gupta, C. Gupta, S. Sharma, B. Rathi, R. K. Sharma, and H. B. Bohidar, *RSC Adv*ances, **6**, No. 112: 111099 (2016); https://doi.org/10.1039/C6RA24586B
57. S. T. Navale, D. K. Bandgar, S. R. Nalage, G. D. Khuspe, M. A. Chougule, Y. D. Kolekar, S. Sen, and V. B. Patil, *Ceramics International*, **39**, No. 6: 6453 (2013); https://doi.org/10.1016/j.ceramint.2013.01.074
58. J. Huang, M. Yang, C. Gu, M. Zhai, Y. Sun, and J. Liu, *Materials Research Bulletin*, **46**, No. 8: 1211 (2011); https://doi.org/10.1016/j.materresbull.2011.04.004
59. D. Su, K. Hyun-Soo, K. Woo-Seong, and G. Wang, *Microporous and Mesoporous Materials*, **149**, No. 1: 36 (2012); https://doi.org/10.1016/j.micromeso.2011.09.002
60. J. Lian, X. Duan, J. Ma, P. Peng, T. Kim, and W. Zheng, *ACS Nano*, **3**, No. 11: 3749 (2009); https://doi.org/10.1021/nn900941e